

# A Novel Sandwich-Type Electrochemical Immunosensor Based on the Signal Amplification Strategy of Core-shell Pd@Pt Nanoparticles for $\alpha$ -fetoprotein Detection

Ke Zhang<sup>1,#</sup>, Zhiwen Cao<sup>1,#</sup>, Shaozhen Wang<sup>1,2</sup>, Jiexia Chen<sup>1</sup>, Yan Wei<sup>1,2,\*</sup>, Dexiang Feng<sup>1,2,\*</sup>

<sup>1</sup> Department of Chemistry, Wannan Medical College, Wuhu, 241002, China

<sup>2</sup> Institute of Synthesis and Application of Medical Materials, Department of Pharmacy, Wannan Medical College, Wuhu, 241002, China

\*E-mail: [yanwei@wnmc.edu.cn](mailto:yanwei@wnmc.edu.cn) ; [fengdxiang@163.com](mailto:fengdxiang@163.com)

#These authors contributed equally to this work

Received: 22 October 2019 / Accepted: 27 December 2019 / Published: 10 February 2020

---

In this work, a novel sandwich-type electrochemical immunosensor capable of detecting  $\alpha$ -fetoprotein (AFP) was fabricated. In this process, the gold nanoparticles with unique biological and electrical properties were used as the substrate material for the immobilization of primary antibodies. Meanwhile, the as-obtained core-shell Pd@Pt nanoparticles-thionine composites with good biocompatibility and high indexed facets were selected as the label of signal antibodies towards hydrogen peroxide (H<sub>2</sub>O<sub>2</sub>) reduction to achieve signal amplification. Under the optimized conditions, the immunosensor for the detection of AFP exhibited a suitable linear response from 0.1 pg mL<sup>-1</sup> to 100 ng mL<sup>-1</sup> with a low detection limit of 0.035 pg mL<sup>-1</sup> (S/N = 3). Moreover, the immunosensor also showed acceptable stability, reproducibility and specificity, implying its potential application in bioassay analysis.

---

**Keywords:** Alpha-fetoprotein; Immunosensor; Gold nanoparticles; Core-shell Pd@Pt nanoparticles

## 1. INTRODUCTION

$\alpha$ -Fetoprotein (AFP) is a significant tumor marker, which could express in primary liver cancer [1-3]. The serum AFP level is less than 25 ng mL<sup>-1</sup> in healthy adult but increases rapidly in patients with original liver carcinoma [4,5]. As a consequence, the quantitative detection of AFP play a vital role in screening and diagnosis of liver cancer. Thus, it is critical to establish an accurate and convenient approach for the determination of AFP. Recently, sandwich-type electrochemical immunosensors have garnered extensive attention due to their advantages of fast response, excellent selectivity, ease of handling and high sensitivity [6-11].

For the sandwich-type electrochemical immunosensors, a crucial issue of detection is to integrate various superior catalytic and appropriate stable nanomaterials with secondary antibodies ( $Ab_2$ ) to achieve signal amplification. According to reports, some metal nanoparticles (NPs) such as PdNPs, PtNPs, RuNPs and some other noble metal nanoparticles exhibited highly catalytic behavior towards  $H_2O_2$  reduction [12-14]. Among these, PdNPs and PtNPs were considered as better catalysts owing to their good biocompatibility, conductivity and high sensitivity towards  $H_2O_2$  [12]. For example, Li et al. employed  $Zn_2SiO_4$ -PdNPs units as a secondary amplification path for the detection of insulin [15]. Chang et al. synthesized PtNPs@PS and exploited its application in bioanalysis [16]. In comparison with monometallic nanoparticles, Pt/Pd and other noble bimetallic nanoparticles often showed stronger catalytic activity and stability because of the synergistic interaction of the two metals [17-21]. Moreover, bimetallic nanoparticles with core-shell structure has large inter-connecting area and abundant active sites, leading to immobilization of plenty of  $Ab_2$  [22-24]. Naturally, the core-shell Pd@Pt nanoparticles showed superior catalytic activity and good chemical stability, which also acted as an ideal candidate for biosensing design.

Here we construct a novel immunosensor using gold nanoparticles (AuNPs) as the electrode material and AFP antibodies-Pd@Pt nanoparticles-thionine conjugates as signal tags. The AuNPs not only can improve electrical conductivity, but also can afford a satisfactory electrochemical sensing platform for immobilizing primary antibodies [3,25-30]. Meanwhile, the core-shell Pd@Pt nanoparticles-thionine composites utilized as the label of  $Ab_2$ , which could generate signals by themselves and serve as catalyst without the additional modification of electroactive substance and catalyst. It can greatly shorten the analysis time. Additionally, the Pd@Pt bimetallic nanoparticles could be used to catalyze the  $H_2O_2$  reaction, enhancing the current signals to realize the signal amplification. The constructed immunosensor exhibits a good performance in real samples detection, suggesting great potential for the bioanalytical applications.

## 2. EXPERIMENTAL

### 2.1. Materials and Apparatus

Anti-AFP ( $Ab_1$ ,  $Ab_2$ ) and AFP from Biocell Biotech Co., Ltd. Thionine (Thi), bovine serum albumin (BSA),  $K_2PdCl_4$ ,  $H_2PtCl_4$ ,  $NaH_2PO_4$ , HEPES, Urea,  $Na_2HPO_4$ , KCl, Hydrogen peroxide ( $H_2O_2$ ) and chloroauric acid ( $HAuCl_4 \cdot 4H_2O$ ) were obtained from the Sinopharm Chemical Reagent Co., Ltd. All reagents used were of analytical grade. The three-electrode system included an Au working electrode, a saturated calomel reference electrode, and an auxiliary platinum electrode. Electrochemical impedance spectroscopy (EIS) and differential pulse voltammetry (DPV) measurements were conducted on a CHI-660E electrochemical workstation (Shanghai CH Instruments Co., China). Scanning electron microscopy (SEM) was recorded with JSM-7100F (Japan Electron, Japan) with transmission electron microscopy (TEM) on JEM-6700F (Japan Electron, Japan).

## 2.2. Preparing the Palladium nanoseeds

Briefly, 1 mL of  $\text{K}_2\text{PdCl}_4$  ( $10 \text{ mmol mL}^{-1}$ ), 1 mL of Urea ( $0.1 \text{ mmol mL}^{-1}$ ), 14 mL of HEPES ( $10 \text{ mmol mL}^{-1}$ ) and 2 mL ultrapure water were placed in an autoclave and heated with 3 h at  $120 \text{ }^\circ\text{C}$ . Subsequently, it was cooled to ambient temperature. Finally, the mixed solution was centrifuged ( $10000 \text{ rpm}$ , 8 min) and washed with ultrapure water.

## 2.3. Preparing the core-shell Pd@Pt nanoparticles

The Pd@Pt nanoparticles were prepared following a literature procedure with some modification [31]. The above 8 mL of palladium nanoseeds solution and  $100 \text{ }\mu\text{L}$  of ascorbic acid ( $0.1 \text{ mol mL}^{-1}$ ) were mixed together with  $0.8 \text{ mL}$  of  $\text{H}_2\text{PtCl}_4$  ( $10 \text{ mmol mL}^{-1}$ ). The resulting mixture was placed in an autoclave and heated at  $140 \text{ }^\circ\text{C}$  for 4 hours. The resultant black solution was cooled to ambient temperature. The precipitate was centrifuged ( $8000 \text{ rpm}$ , 5 min) and purified with ethanol for three times.

## 2.4. Preparing the Pd@Pt-Thi-Ab<sub>2</sub> bioconjugates

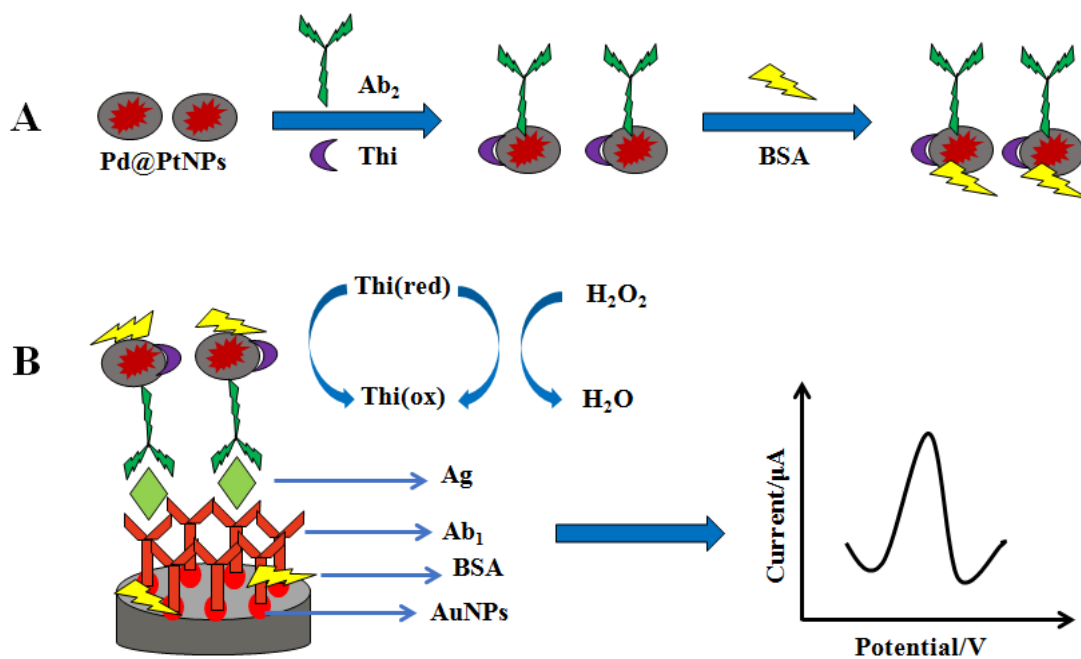
The  $250 \text{ }\mu\text{L}$  of Ab<sub>2</sub> ( $10 \text{ mg mL}^{-1}$ ) and 10 mg of Thi were added into the above Pd@Pt solution and continually shaken at  $4 \text{ }^\circ\text{C}$ . After 6 hours, the composites were centrifuged ( $8000 \text{ rpm}$ , 5 min) and washed with PBS (pH 6.0). Eventually, the bioconjugates were redispersed in blocking solution (0.25 wt% BSA) and preserved at  $4 \text{ }^\circ\text{C}$ . The preparation procedure of the Pd@Pt-Thi-Ab<sub>2</sub> bioconjugates is shown in Scheme 1A.

## 2.5. Fabrication of the immunosensor

Before every use of Au electrodes (AuE), they were pretreated with  $0.05 \text{ }\mu\text{m}$  alumina powder. AuNPs were electrochemically deposited on the cleaned AuE by applying  $-250 \text{ mV}$  for 50 s in  $5.0 \text{ mM mL}^{-1}$   $\text{HAuCl}_4$  solution. Afterwards,  $6 \text{ }\mu\text{L}$  of Ab<sub>1</sub> ( $200 \text{ }\mu\text{g mL}^{-1}$ ) was dropped on the AuE for 12 hours. And then, the AuE was blocked with  $6 \text{ }\mu\text{L}$  BSA (1.0 wt%) for 40 min at  $37 \text{ }^\circ\text{C}$ . Scheme 1B reveals the construction process of the immunosensor.

## 2.6. Determination of AFP

Before measurement, the as-prepared electrode was incubated with  $6 \text{ }\mu\text{L}$  AFP solution of multiple concentrations at  $37 \text{ }^\circ\text{C}$ . After rinse, the electrode was incubated in Pd@Pt-Thi-Ab<sub>2</sub> bioconjugates at  $37 \text{ }^\circ\text{C}$  for 50 min. Finally, the obtained electrode was investigated by DPV in PBS (pH 6.0) with  $4 \text{ mmol L}^{-1}$   $\text{H}_2\text{O}_2$ . The measurement parameters are listed: potential window,  $-0.4$  to  $0 \text{ V}$ ; potential amplitude,  $50 \text{ mV}$ .



**Scheme 1.** (A) Preparation procedure of the Pd@Pt-Thi-Ab<sub>2</sub> bioconjugates. (B) Construction of the Pd@Pt-Thi-Ab<sub>2</sub>/Ag/BSA/Ab<sub>1</sub>/AuNPs/AuE and measurement principle.

### 3. RESULTS AND DISCUSSION

#### 3.1. Characterization of AuNPs and core-shell Pd@Pt nanoparticles

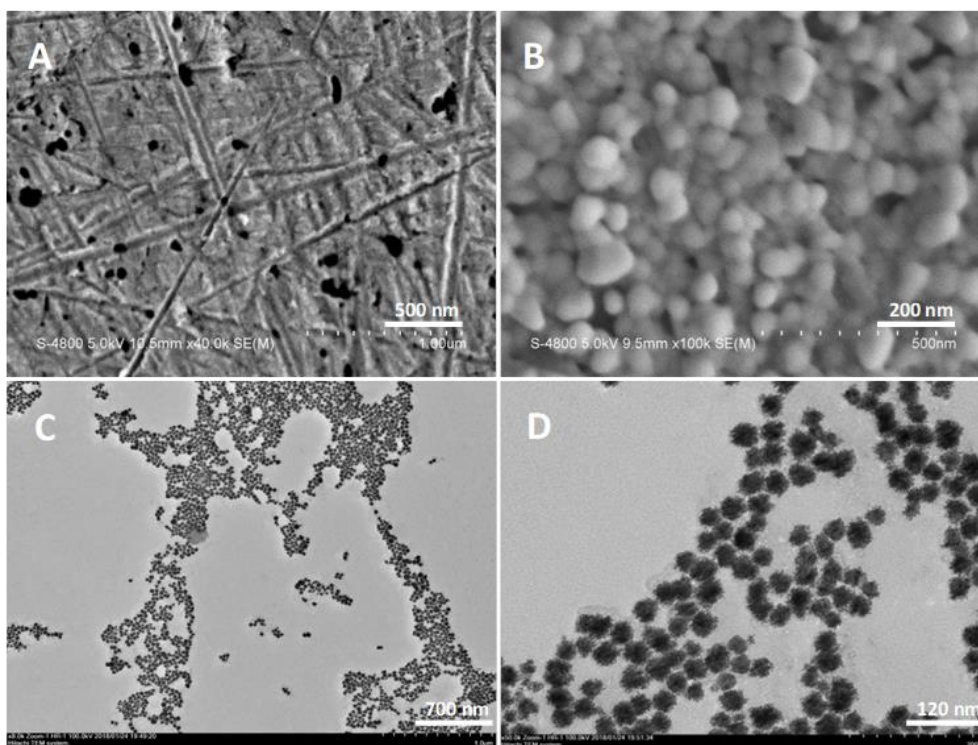


**Figure 1.** SEM images of bare AuE (A) and AuNPs (B). TEM images of Pd@Pt nanoparticles (C, D).

The SEM images of the bare AuE and AuNPs are presented in Fig. 1(A and B). It can be seen that the surface of the bare AuE was not smooth (Fig. 1A). By electrodeposition, a homogeneous coverage of AuNPs on the surface of electrode can be seen, shown in Fig. 1B, indicating that AuNPs were effectively immobilized on the AuE. The well-distributed AuNPs can obtain remarkable biological compatibility and good conductivity of the immunosensor [28,29]. The morphologies of the Pd@Pt nanoparticles were characterized by TEM (Fig. 1C and 1D). Clearly, the prepared Pd@Pt nanoparticles have formed uniform spherical morphology, with an average diameter of 30 nm. As shown in Fig. 1D, the Pd@Pt nanoparticles showed a core-shell structure, which could provide a large inter-connecting area and many active sites for catalytic reactions [31].

### 3.2. EIS of the immunosensor

EIS was used to evaluate the electronic transfer properties of immunosensing process. As shown in Fig. 2, the unmodified AuE exhibited a relatively small interfacial resistance (curve a). When a film of AuNPs was fixed on the AuE (curve b), the interfacial resistance shorten obviously, this might be caused by the unique conductivity of AuNPs, which accelerated fast electron transfer process [28]. However, the interfacial resistance increased gradually when the AuE was coated with Ab<sub>1</sub>, BSA and AFP in due succession (curve c, d and e), the reason is that these bioactive substances perturbed the interfacial and retarded the electron transfer [3]. Subsequently, the interfacial resistance decreased significantly when the Pd@Pt-Thi-Ab<sub>2</sub> bioconjugates (curve f) were assembled, indicating that the bioconjugates had a high electrical transport properties. All these observations proved that AuNPs, Ab<sub>1</sub>, BSA, AFP and Pd@Pt-Thi-Ab<sub>2</sub> bioconjugates have been successfully fastened at the AuE.

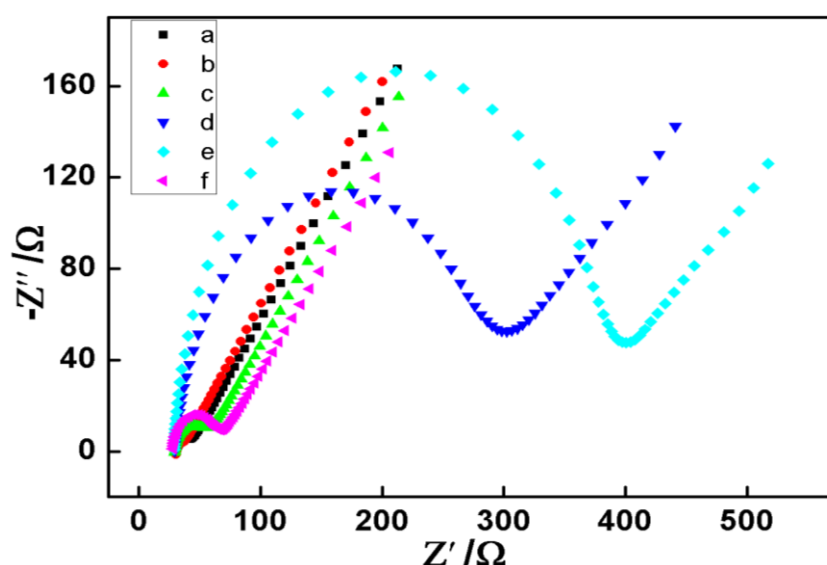


**Figure 2.** EIS of (a) bare AuE, (b) AuNPs/AuE, (c) Ab<sub>1</sub>/AuNPs/AuE, (d) BSA/Ab<sub>1</sub>/AuNPs/AuE, (e) Ag/BSA/Ab<sub>1</sub>/AuNPs/AuE and (f) Pd@Pt-Thi-Ab<sub>2</sub>/Ag/BSA/Ab<sub>1</sub>/AuNPs/AuE in 5.0 mmol L<sup>-1</sup> [Fe(CN)<sub>6</sub>]<sup>3-/4-</sup> and 0.1 mol L<sup>-1</sup> KCl solution.

### 3.3. Optimal parameters

To achieve the best performance, the fluence of Ab<sub>2</sub> incubation time was systematically studied in the time periods from 20 to 60 min (Fig. 3A). The DPV response increased rapidly within the first 50 min and then decreased. Thus, 50 min was used throughout this experiment. By the same token, the effect of pH value of PBS was also investigated (Fig. 3B). The DPV response enhanced with the increasing of pH value from 5.0 to 6.0, while decreased with further increasing pH value. Therefore, PBS pH at 6.0 was selected for the immunoassay.

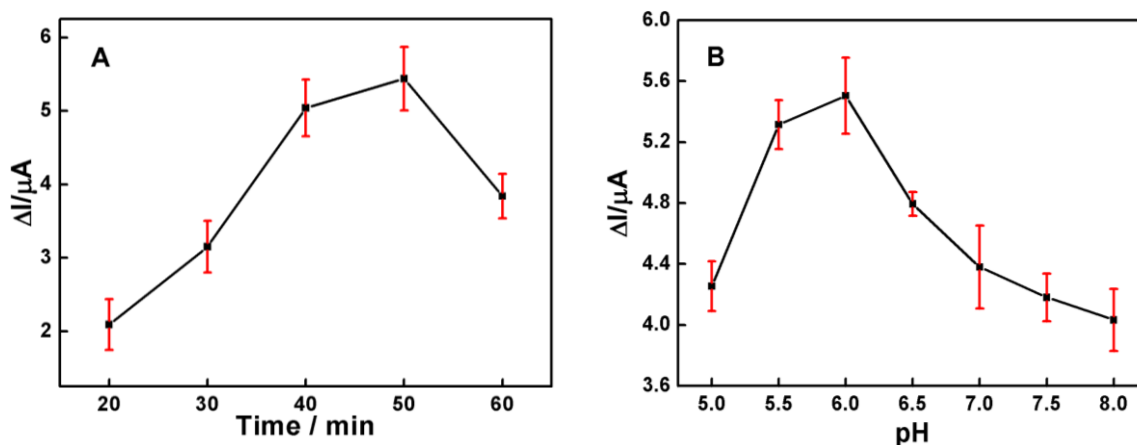


**Figure 3.** Effects of (A) incubation time of Ab<sub>2</sub>, (B) pH of PBS on the immunosensor.

### 3.4. Electrocatalytic behavior

Under the experimental parameters, we investigated the detectability of the immunosensor. Fig. 4 reveals the DPV peaks for various concentrations of AFP (0, 0.0001, 0.001, 0.01, 0.1, 0.5, 1, 5, 10 and 100 ng mL<sup>-1</sup>). The DPV peaks showed stepped increases, which suggests a wide linear range for AFP detection. The linear equation was  $y = 5.1557 + 0.9576x$ , where  $R^2$  was 0.993. The limit of detection was 0.035 pg mL<sup>-1</sup> (S/N = 3). Table 1 shows a comparison of the proposed immunosensor in this work with other noble metal modified AFP immunosensors. It can be seen that the proposed immunosensor shows excellent performance for both linear range and detection limit, which may be attributed to the following factors. Firstly, the AuNPs with remarkable electroconductibility and biocompatibility can ensure the electron transfer towards the surface of the electrode and the successful conjugation of Ab<sub>1</sub> [3,27,29]. Secondly, the Pd@Pt core-shell nanoparticles possess extraordinary biocompatibility to load Ab<sub>2</sub>, and more importantly, they possess excellent catalytic activity and good electron transfer capability, which is an important performance for electrochemical immunosensors [31].

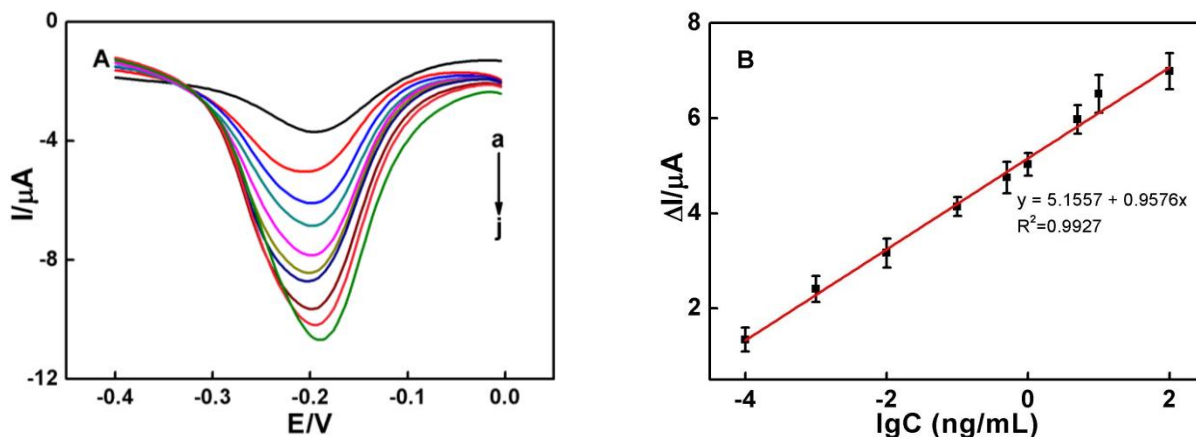


**Figure 4.** (A) DPV signals of the immunosensor in the presence of 0, 0.0001, 0.001, 0.01, 0.1, 0.5, 1, 5, 10 and 100 ng mL<sup>-1</sup> AFP (a~j) in PBS (pH 6.0). (B) Calibration plots of the peak current ( $\Delta I$ ) vs the logarithmic concentration of AFP.

**Table 1.** Comparison of analytical characteristics of various immunosensors for AFP

Electrode	Detection limit	Linear range	Refs
poly(MB)-Au/GCE	0.0196 pg mL <sup>-1</sup>	0.001-100 ng mL <sup>-1</sup>	[3]
GNPs/GCE	40 pg mL <sup>-1</sup>	0.1-200 ng mL <sup>-1</sup>	[5]
Pd/GCE	4 pg mL <sup>-1</sup>	0.01-75 ng mL <sup>-1</sup>	[10]
PtNPs@PS-DNA/AuNPs/GCE	0.086 pg mL <sup>-1</sup>	0.0001-100 ng mL <sup>-1</sup>	[16]
AuNPs/Fc-IL-CHO/AuNPs-PAMAM/AuE	20 pg mL <sup>-1</sup>	0.05-30 ng mL <sup>-1</sup>	[32]
graphene/Au-Pd/GCE	5 pg mL <sup>-1</sup>	0.05-30 ng mL <sup>-1</sup>	[33]
AuNPs-HRP/Thi-Chit/GCE	0.03 pg mL <sup>-1</sup>	0.0001-10 ng mL <sup>-1</sup>	[34]
Au-PDA-PB-GO/GCE	7 pg mL <sup>-1</sup>	0.01-80 ng mL <sup>-1</sup>	[35]
PIn-5-COOH/MWCNTs-COOH/GCE	0.033 pg mL <sup>-1</sup>	0.001-100 ng mL <sup>-1</sup>	[36]
Pd@Pt-Thi/AuE	0.035 pg mL <sup>-1</sup>	0.0001-100 ng mL <sup>-1</sup>	Present Work

Poly(MB)-Au, poly(methylene blue)-Au nanocomposites; GCE, glassy carbon electrode; GNPs, gold nanorods; Pd, Pd nanoplates; PtNPs, Pt nanoparticles; PS, polymer nanospheres; DNA, DNAzyme; IL, ionic liquids; CHO, aldehyde groups; PAMAM, polyamidoaminic dendrimers; AuE, Au electrode; Au-Pd, Au-Pd nanoparticles, HRP, horseradish peroxidase; Thi-Chit, thionine and chitosan; PDA, polydopamine; GO, graphene oxide; PIn-5-COOH, indole-5-carboxylic acid.

### 3.5. Specificity, stability and reproducibility

To evaluate the specificity of the proposed immunosensor, some potential interferents (including ascorbic acid (AA), arginine (Arg), BSA and carcino-embryonic antigen (CEA); each 50 ng mL<sup>-1</sup>) and these potential interferents with AFP solutions (10 ng mL<sup>-1</sup>) have been measured by DPV. The DPV responses of pure interferents were negligible compared with that of pure AFP (Fig. 5).

Furthermore, the DPV responses of pure AFP did not appear remarkable difference with the hybrid samples. All these indicated that the proposed immunosensor possessed remarkable specificity.

The stability of the immunosensor was inspected per five days of storage at 4 °C. After five days, ten days and fifteen days, the DPV responses maintained 97.8 %, 94.4 % and 91.6 % of its initial value respectively. This indicated that the designed immunosensor had suitable stability.

In addition, the reproducibility of the immunosensor was tested by detecting AFP (10 ng mL<sup>-1</sup>) through five equally prepared electrodes. The relative standard deviation (RSD) of those equally prepared electrodes was 3.5 %, implying the good reproducibility of the designed immunosensor.

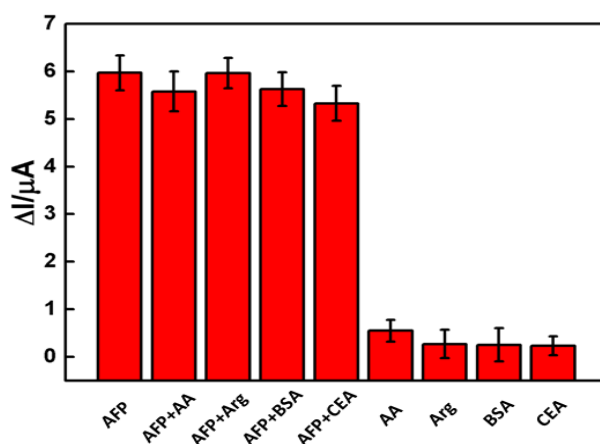


**Figure 5.** Specificity of the immunosensor conditions: C<sub>AFP</sub> = 10 ng mL<sup>-1</sup>; C<sub>interferents</sub> = 50 ng mL<sup>-1</sup> (AA, Arg, BSA and CEA). Error bar = RSD (n = 5).

### 3.6. Practical applications

**Table 2.** Determination of AFP in human serum samples by the immunosensor

sample	Added (ng mL <sup>-1</sup> )	Found (ng mL <sup>-1</sup> )	Recovery (%)
1	0.5	0.52	104.0
2	5.0	5.3	106.0
3	10	11.3	113.0
4	40	39.1	97.8
5	80	77.2	96.5

The analytical reliability of the immunosensor was assessed by measuring various AFP concentrations in human serum. Standard addition method was used for the analysis. As 0.5, 5.0, 10, 40 and 80 ng mL<sup>-1</sup> AFP were added to samples respectively, the recovery rate ranged from 96.5 % to 113.0 % (Table 2). This result demonstrated that our proposed method provides promising potential for AFP detection in disease diagnostics.



#### 4. CONCLUSIONS

Herein, a highly sensitive immunosensor was fabricated for electrochemical immunoassay of AFP. AuNPs as the substrate material were used to effectually capture antibodies. The core-shell Pd@Pt nanoparticles as the current signal amplifier provide many active sites for loading secondary antibodies and catalyzing H<sub>2</sub>O<sub>2</sub> reduction to effectively amplify the response signal. Furthermore, the proposed method also could accurate detection of AFP in real samples. Therefore, this offers a new promising platform for determining other tumor markers in clinic.

#### ACKNOWLEDGEMENTS

The authors would like to acknowledge financial support from the Provincial Foundation for Academic and Technical Leaders Reserve Candidate of Anhui Province (2016H086), the Research Fund for University Natural Science Research Project of Anhui Province (KJ2018A0257, KJ2019A0414), and the Excellent Young Talents Fund Program of Higher Education Institutions of Anhui Province (gxyq2018043).

#### References

1. D. Sun, H. Li, M. Li, C. Li, L. Qian, B. Yang, *Biosens. Bioelectron.*, 132(2019)68.
2. M. D. A. Fabio Conti, Annagiulia Gramenzi, Maurizio Biselli, *Biomark. Med.*, 9(2015) 1343.
3. J. Shan, L. Wang, Z. Ma, *Sensors and Actuators B: Chemical*, 237(2016)666.
4. S. Zhang, C. Zhang, Y. Jia, X. Zhang, Y. Dong, X. Li, Q. Liu, Y. Li, Z. Zhao, *Bioelectrochemistry*, 128(2019)140.
5. C. Zhou, D. Liu, L. Xu, Q. Li, J. Song, S. Xu, R. Xing, H. Song, *Sci. Rep.*, 5(2015)9939.
6. M. Li, P. Wang, F. Pei, H. Yu, Y. Dong, Y. Li, Q. Liu, P. Chen, *Sensors and Actuators B: Chemical*, 261(2018)22.
7. Y. Zheng, H. Wang, Z. Ma, *Microchimica Acta*, 184(2017)4269.
8. Q. Yan, L. Cao, H. Dong, Z. Tan, Q. Liu, W. Zhang, P. Zhao, Y. Li, Y. Liu, Y. Dong, *Anal. Chim. Acta.*, 1069(2019)117.
9. Y. Yang, *International Journal of Electrochemical Science*, 14 (2019)4095.
10. H. Wang, H. Li, Y. Zhang, Q. Wei, H. Ma, D. Wu, Y. Li, Y. Zhang, B. Du, *Biosens. Bioelectron.*, 53(2014)305.
11. S. Yin, Z. Ma, *Biosens. Bioelectron.*, 140(2019)111355.
12. X. Zhou, X. Qian, X. Tan, X. Ran, Z. Li, Z. Huang, L. Yang, X. Xie, *Anal. Chim. Acta.*, 1068(2019)18.
13. S. Gupta, A. Tiwari, U. Jain, N. Chauhan, *Mater. Sci. Eng. C. Mater. Biol. Appl.*, 103(2019)109733.
14. M. S. Khan, W. Zhu, A. Ali, S. M. Ahmad, X. Li, L. Yang, Y. Wang, H. Wang, Q. Wei, *Anal. Biochem.*, 566(2019)50.
15. Y. Li, L. Tian, L. Liu, M. S. Khan, G. Zhao, D. Fan, W. Cao, Q. Wei, *Talanta*, 179(2018)420.
16. H. Chang, H. Zhang, J. Lv, B. Zhang, W. Wei, J. Guo, *Biosens. Bioelectron.*, 86(2016)156.
17. J. Wu, J. He, C. Zhang, J. Chen, Y. Niu, Q. Yuan, C. Yu, *Biosens. Bioelectron.*, 102(2018)403.
18. F. Zhu, G. Zhao, W. Dou, *Anal. Biochem.*, 559(2018)34.
19. C. Wang, Q. Tang, K. Zhao, A. Deng, J. Li, *Analyst*, 144(2019)1590.
20. Y. Yang, Q. Yan, Q. Liu, Y. Li, H. Liu, P. Wang, L. Chen, D. Zhang, Y. Li, Y. Dong, *Biosens. Bioelectron.*, 99(2018)450.
21. R. Wang, A. J. Wang, W. D. Liu, P. X. Yuan, Y. Xue, X. Luo, J. J. Feng, *Biosens. Bioelectron.*,

- 102(2018)276.
22. X. Xiao, H. Jeong, J. Song, J. P. Ahn, J. Kim, T. Yu, *Chem. Commun (Camb)*, 55(2019)11952.
  23. M. S. Khan, H. Ameer, A. Ali, R. Manzoor, L. Yang, R. Feng, N. Jiang, Q. Wei, *Biosens. Bioelectron.*, 147(2020)111767.
  24. B. He, S. Yan, *Mikrochim. Acta*, 186(2019)77.
  25. G. Luo, *International Journal of Electrochemical Science*, (2019)8419.
  26. X. X. Dong, J. Y. Yang, L. Luo, Y. F. Zhang, C. Mao, Y. M. Sun, H. T. Lei, Y. D. Shen, R. C. Beier, Z. L. Xu, *Biosens. Bioelectron.*, 98(2017)305.
  27. T. Yang, Y. Gao, Z. Liu, J. Xu, L. Lu, Y. Yu. *Sensors and Actuators B: Chemical*.239(2017)76.
  28. V. Serafin, R. M. Torrente-Rodriguez, A. Gonzalez-Cortes, P. Garcia De Frutos, M. Sabate, S. Campuzano, P. Yanez-Sedeno, J. M. Pingarron, *Talanta*, 179(2018)131.
  29. Q. Rong, H. Han, F. Feng, Z. Ma, *Sci. Rep.*, 5(2015)11440.
  30. Z. Song, R. Yuan, Y. Chai, B. Yin, P. Fu, J. Wang, *Electrochimica. Acta*, 55(2010)1778.
  31. H. Ataee-Esfahani, M. Imura, Y. Yamauchi, *Angew. Chem. Int. Ed. Engl.*, 52(2013)13611.
  32. Y. Shen, G. Shen, Y. Zhang, *Mikrochim. Acta.*, 185(2018)346.
  33. L. Zhao, S. Li, J. He, G. Tian, Q. Wei, H. Li, *Biosens. Bioelectron.*, 49(2013)222.
  34. D. Lu, Q. Xu, G. Pang, F. Lu, *Biomed. Microdevices*, 20(2018)46.
  35. T. Yang, X. Ren, M. Yang, X. Li, K. He, A. Rao, Y. Wan, H. Yang, S. Wang, Z. Luo, A highly sensitive label-free electrochemical immunosensor based on poly(indole-5-carboxylic acid) with ultra-high redox stability, *Biosens. Bioelectron.*, 141(2019)111406.
  36. R. Zhang, B. Pan, H. Wang, J. Dan, C. Hong, H. Li, Polydopamine and graphene oxide synergistically modified Prussian blue electrochemical immunosensor for the detection of alpha-fetoprotein with enhanced stability and sensibility, *RSC. Advances.*, 48 (2015)38176.